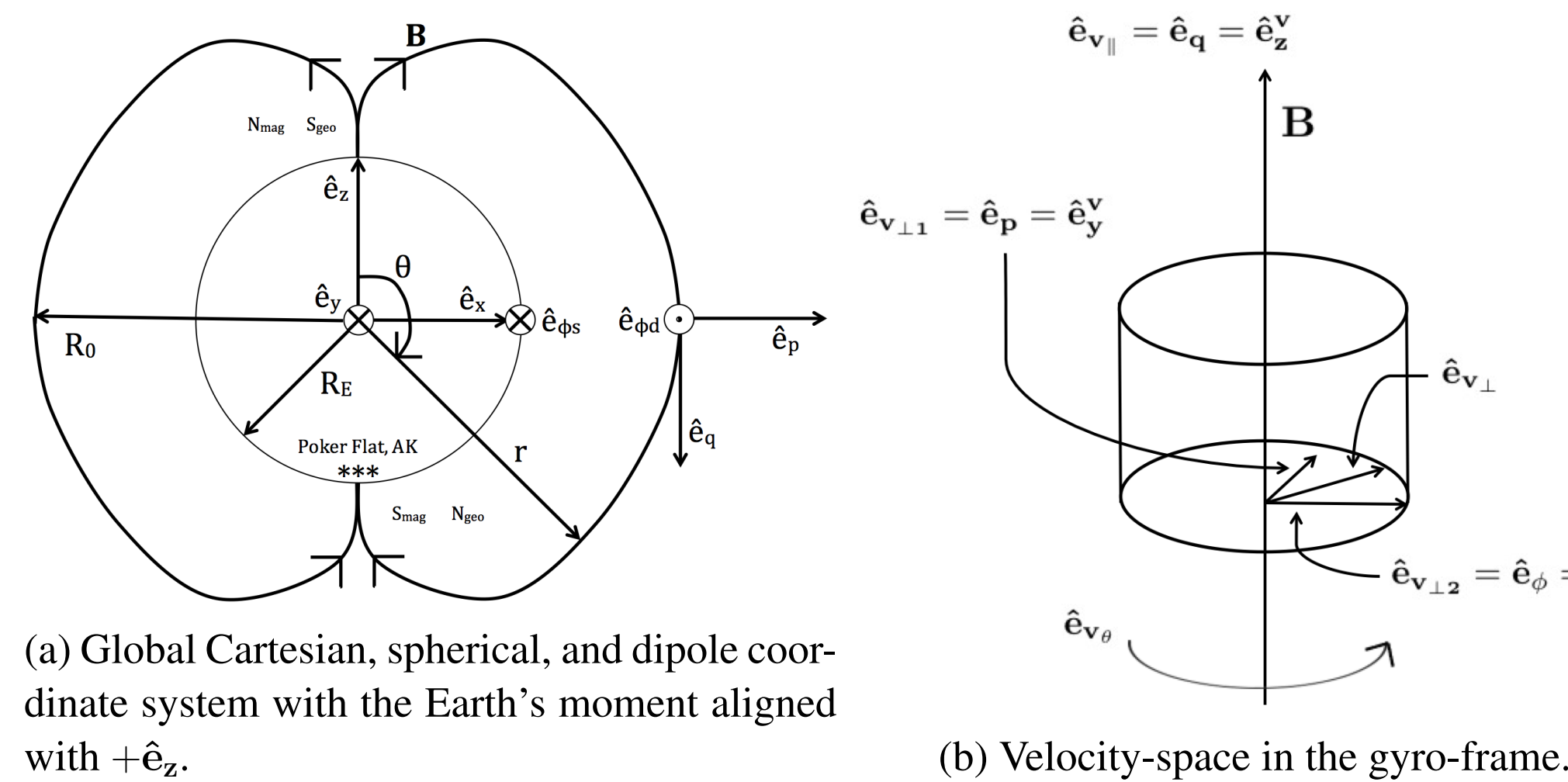


¹Department of Atmospheric and Oceanic Sciences, University of California, Los Angeles, CA, USA ²Department of Physical Sciences, Embry-Riddle Aeronautical University, Daytona Beach, FL, United States ³NASA Goddard Space Flight Center, Greenbelt, MD, United States ⁴Physics Department, The University of New Hampshire, Durham, NH, United States

Plasma escape from the high-latitude ionosphere (ion outflow) serves as a significant source of heavy plasma to magnetospheric plasma sheet and ring current regions. Outflows alter mass density and reconnection rates, hence global responses of the magnetosphere. A new fully kinetic and semi-kinetic model is constructed from first principles which traces large numbers of individual O⁺ ion macro-particles along curved magnetic field lines, using a guiding-center approximation, in order to facilitate calculation of ion distribution functions and moments. Particle forces include mirror and parallel electric field forces, a self-consistent ambipolar electric field, and a parameterized source of ion cyclotron resonance (ICR) wave heating, thought to be central to the transverse energization of ions. The model is initiated with a steady-state ion density altitude profile and Maxwellian velocity distribution and particle trajectories are advanced via a direct simulation Monte Carlo (DSMC) scheme. This outlines the implementation of the kinetic outflow model, demonstrates the model's ability to achieve near-hydrostatic equilibrium necessary for simulation spin-up, and investigates L-shell dependent wave heating and pressure cookers scenarios. This provides quantitative means to interpret sounding rocket data and related remote sensing approaches to studying ion outflows and serves to advance our understanding of the drivers and particle dynamics in the auroral ionosphere and to improve data analysis for future sounding rocket and satellite missions.

INTRODUCTION & MOTIVATION

Ionospheric outflow at polar latitudes has been avid subject of study since predicted [Dessler & Michel, 1966] [Nishida, 1966]. First evidence of ionospheric plasma populating magnetosphere inferred by precipitating keV O⁺ fluxes exceeding H⁺ fluxes [Shelley et al., 1976]. It is well known that O⁺ is dominant up to 4000-7000 km [Yau et al., 2007, 2012]. Heavy ionospheric ions in magnetosphere can affect [Lin et al., 2020]: 1) wave propagation [Bashir & Ilie, 2018] [Keika et al., 2011] [Summers & Thorne, 2003] [Summers et al., 2007], 2) reconnection rates by mass loading [Garcia et al., 2010] [Nosé et al., 2005] [Winglee et al., 2002] [Wiltberger et al., 2010], 3) ring current dynamics [Daglis et al., 1999] [Hamilton et al., 1988] [Kistler et al., 1989] [Liemohn et al., 1999], 4) cross polar cap potential (CPCP) [Glocer et al., 2009] [Ilie et al., 2013] [Winglee et al., 2002]. Type 1 ion upflow: frictional heating from differential ion-neutral drifts [Wahlund et al., 1992] [Zettergren & Semeter, 2012] with fluxes observed $\sim 8 \times 10^{13} \text{ m}^{-2} \cdot \text{s}^{-1}$ [Wahlund et al., 1992]. Type 2 ion upflow: field-aligned ambipolar electric fields from electrons heated by soft particle precipitation [Su et al., 1999] with fluxes observed $\sim 2.5 \times 10^{14} \text{ m}^{-2} \cdot \text{s}^{-1}$ [Wahlund et al., 1992]. Outstanding questions in ion outflow pressure cooker environments include: How important are the relative roles of BBELF and VLF waves in producing outflows? How low in altitude can energization processes work relative to the collisional transition region? How do pressure cooker environments affect the total outflow in a given region? What are high-altitude non-Maxwellian signatures that may result from acceleration processes at lower altitudes, and how can they be used to diagnose the acceleration mechanisms? This project introduces KAOS (Kinetic model of Auroral ion OutflowS) [Albarran, 2022]. The motivation of KAOS is to construct a model of the ionospheric outflow that: 1) has direct simulation Monte Carlo (DSMC) kinetic and semi-kinetic capabilities, 2) can connect easily to other low-altitude models 3) is flexible enough to handle curved field lines (like many fluid models), and 4) can simulate resonant and non-resonant wave particle interactions. We quantify dependence of upflowing/outflowing ion distributions on: 1) BBELF wave-field transverse wavelength, λ_{\perp} , 2) ion-turbulence interaction time-step, h , 3) reference parallel electric field, $E_{\parallel 0}$, and, 4) simulated altitudes of ionospheric and magnetospheric potential structures.



KINETIC SOLVER

Initial O⁺ ion densities are computed by a thermospheric profile in hydrostatic equilibrium with altitude dependent gravitational acceleration. Ions are initialized temperature isotropic with three-dimensional Maxwellian velocity distribution with standard deviations, $\sigma_i = \sqrt{k_B T_i / m}$, $\forall i = x, y, z$ and transformed to dipole components, where $\hat{e}_{v,1} = \hat{e}_p$ and $\hat{e}_{v,2} = \hat{e}_p$. Translational components follow $v_{\parallel 0} \rightarrow (v_{z0}, v_{y0}, v_{x0})$. Initial transverse velocity components along \hat{e}_p and \hat{e}_ϕ are $v_{\perp 10}$ and $v_{\perp 20}$, respectively. Particle positions and velocities are advanced via RK4 along field lines with gravity, a_G , mirror force, a_M , and self-consistent ambipolar electric fields, E_A , and parallel electric fields, E_{\parallel} , with electrostatic potential drop, $\Delta\Phi_{\parallel}$, for reference parallel electric field, $E_{\parallel 0}$. Lower boundary Maxwellian injection on mean thermal ion transit time through lower boundary ghost cell, $\tau_s = \sqrt{m / (k_B T_i)} h_q(\hat{q}) d_q(\hat{q})|_{\hat{q}=0}$, where $\hat{q} = 0$ is the lower boundary ghost cell index.

$$a_G = \frac{-2GM_{\oplus} \cos(\theta_C)}{r_C^2 \sqrt{r_C}} \hat{e}_q, \quad a_M = \frac{-\mu \partial |B|}{m \partial s} \hat{e}_q, \quad E_A = \frac{k_B T_e \partial n}{q_e n h_q \partial q} \hat{e}_q, \quad E_{\parallel} = \frac{-1 \partial \Delta\Phi_{\parallel}}{h_q \partial q} \hat{e}_q, \quad \Delta\Phi_{\parallel}(\hat{q}) = E_{\parallel 0} \sum_1^{\hat{q}} d_q(\hat{q}) h_q(\hat{q}). \quad (1)$$

Broadband extremely low-frequency (BBELF) and very low-frequency (VLF) wave generation is thought to be driven by suprathermal electron beam instabilities, ion beam instabilities, and velocity shear [Wu et al., 2002] [Ganguli et al., 1994]. Wave heating occurs if the gyro-frequency is larger than the collision frequency and the gyro-radius is smaller than the transverse wavelength, λ_{\perp} , [Wu et al., 2002] [Barakat and Barghouti, 1994] [Bouhran et al., 2003a] [Zeng et al., 2006]. Ion macro-particles are energized by ion cyclotron waves with power spectral density, $S_{\perp}(\omega_g)$, in $[\text{V}^2 \cdot \text{m}^{-2} \cdot \text{Hz}^{-1}]$ left-hand circularly polarized and centered at reference gyro-frequency, ω_{g0} , with spectral index, χ_{\perp} . Wave power is transferred on wave-particle interaction time-scales, $\tau_{\perp} = \sqrt{2\pi ds / (f_g v_{\parallel})}$, where ds is the wave-field field-aligned arc length within frequency bandwidth, Δf , about gyro-frequency, f_g , [Schulz and Lanzerotti, 1974].

Transverse velocities are updated as, $\forall i = 1, 2$,

$$v_{\perp 1}(\tilde{n} + 1) = v_{\perp 1}(\tilde{n}) + \frac{h}{\tau_{\perp 1}} \gamma_{\perp 1} \sqrt{2D_{\perp 1} \tau_{\perp 1}}, \quad v_{\perp 2}(\tilde{n} + 1) = v_{\perp 2}(\tilde{n}) + \frac{h}{\tau_{\perp 2}} \gamma_{\perp 2} \sqrt{2D_{\perp 2} \tau_{\perp 2}},$$

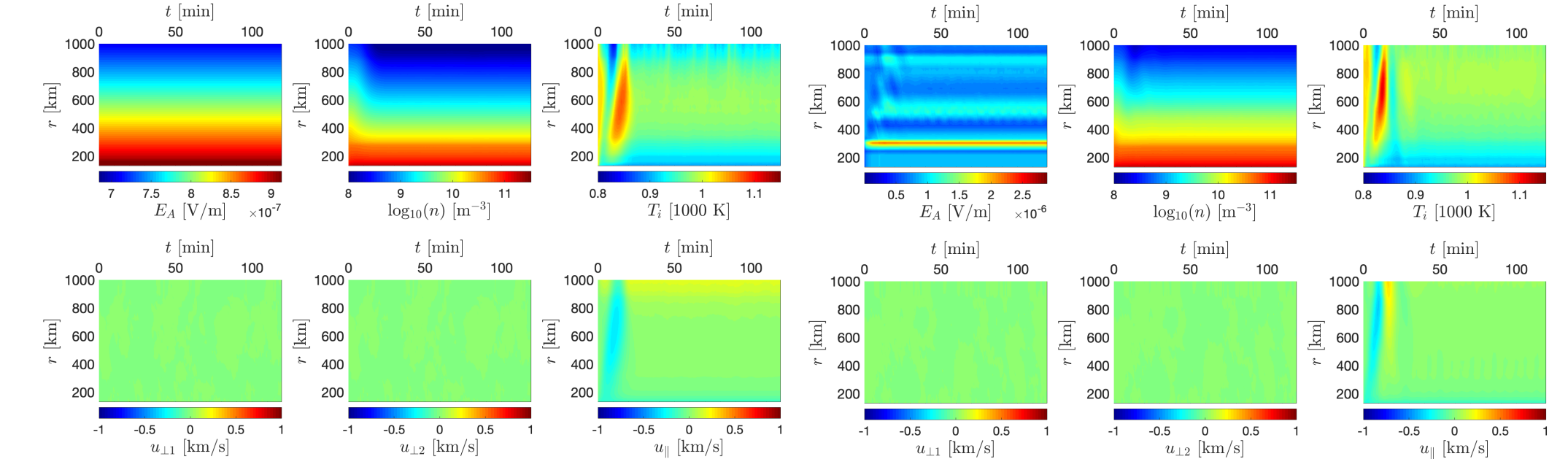
where $\gamma_{\perp 1}, \gamma_{\perp 2} \in N(-1, 1)$ are random numbers from normal distribution functions and transverse velocity diffusion coefficients in units of $[\text{m}^2 \cdot \text{s}^{-3}]$ are, $\forall i = 1, 2$,

$$D_{\perp i} = \sigma_{\perp}^{-3} \left(\frac{q^2}{2m^2} \right) \xi_{\perp i} \eta_{LH} S_0 \left(\frac{\omega_g}{\omega_{g0}} \right)^{-\chi_{\perp i}}, \quad \sigma_{\perp} = \begin{cases} 1 & \text{for } 2\pi\rho_g < \lambda_{\perp} \\ 2\pi v_{\perp 1} / (\lambda_{\perp} \omega_g) & \text{for } 2\pi\rho_g \geq \lambda_{\perp}. \end{cases}$$

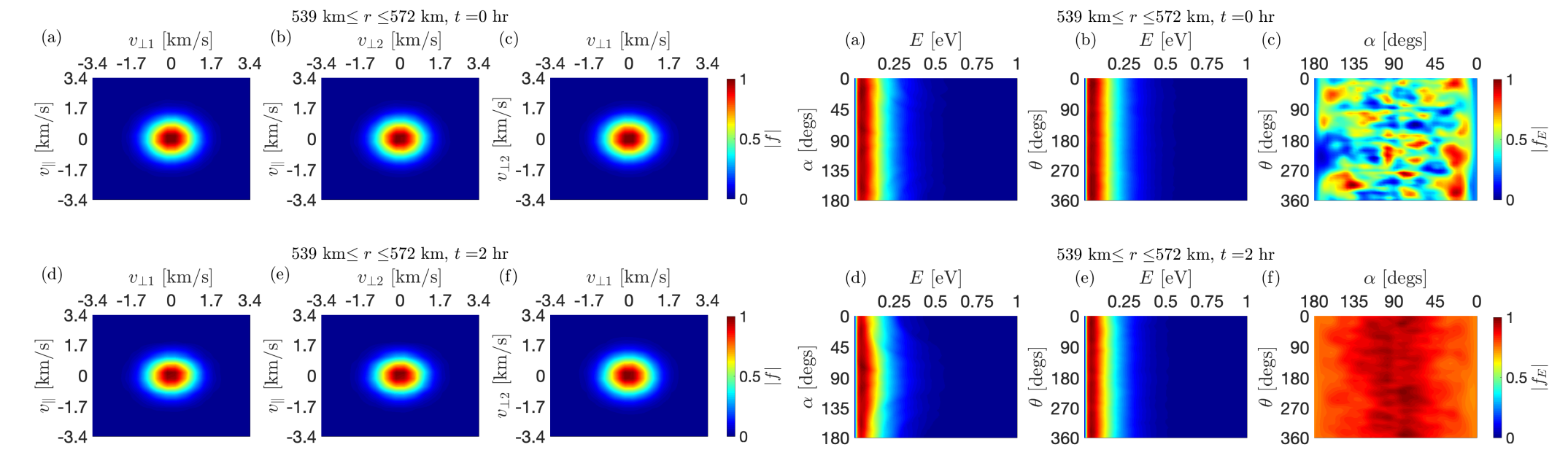
Transverse heating rates are $\dot{W}_{\perp} = m(D_{\perp 1} + D_{\perp 2})$ and $\dot{W}_{\parallel} = 2mD_{\parallel}$ for $D_{\perp 1} = D_{\perp 2}$ [Bouhran et al., 2003a] [Chang and Crew, 1986] [Crew et al., 1990]. Simulation time-steps are selected to resolve the wave-particle interaction time, that is, $h < \tau_{\perp}$.

MODEL EQUILIBRIUM

Static and active ambipolar cases have lower boundary reference density $n_0 = 1 \times 10^{11} \text{ m}^{-3}$ at 133 km, ion temperature $T_i = 1000 \text{ K}$, electron temperature, $T_e = 1500 \text{ K}$, and $L = 8 R_E$. Static ambipolar electric fields take initial density gradients for all time. Self-consistent ambipolar fields drive ions to regions of low density and the system tends closer towards the hydrostatic solution. Kinetic equilibrium in a spin-up simulation is obtained before the introduction of additional particle forcing.

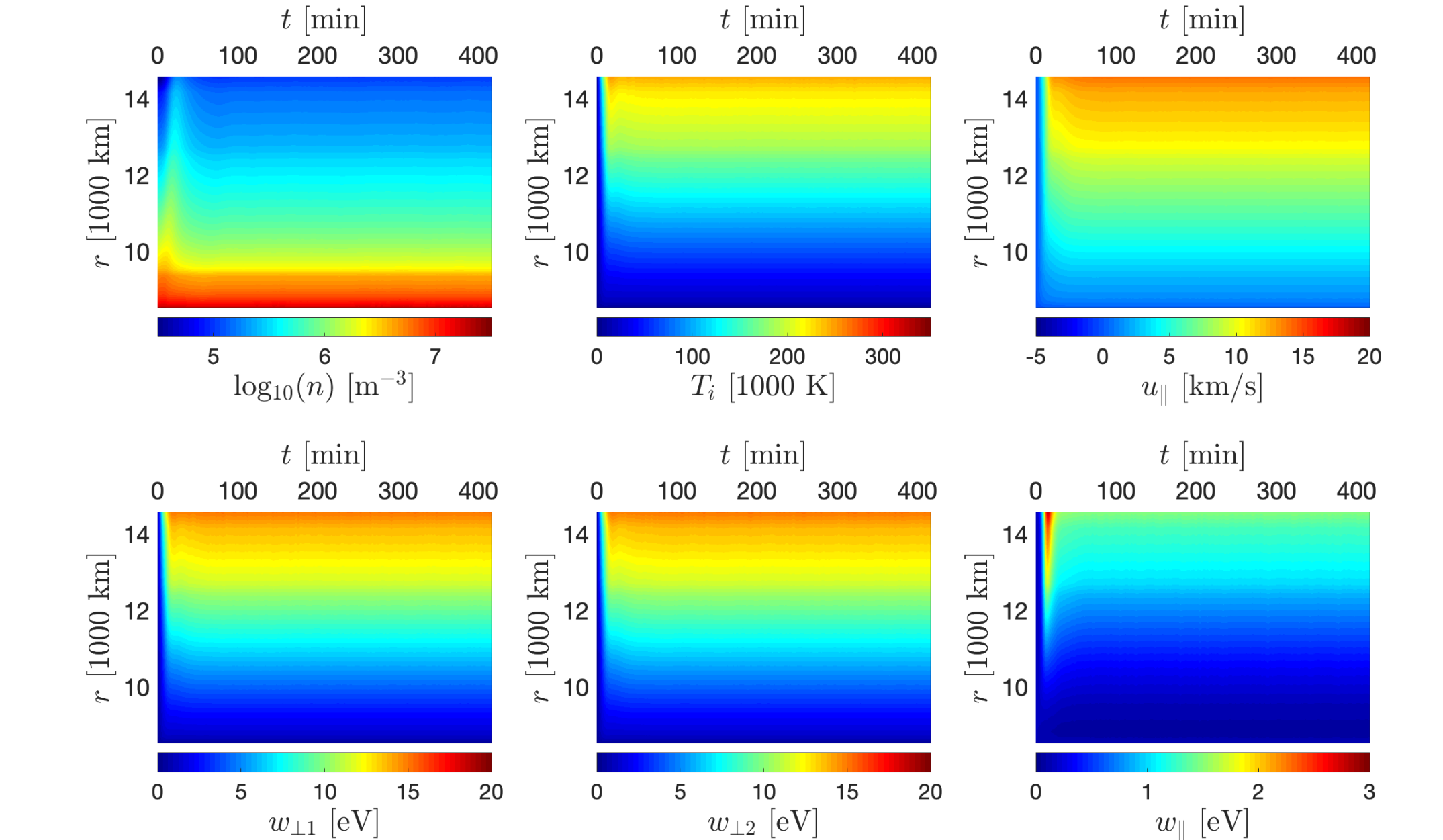


(c) Moments for static ambipolar electric field spin-up. (d) Moments for active ambipolar electric field spin-up.

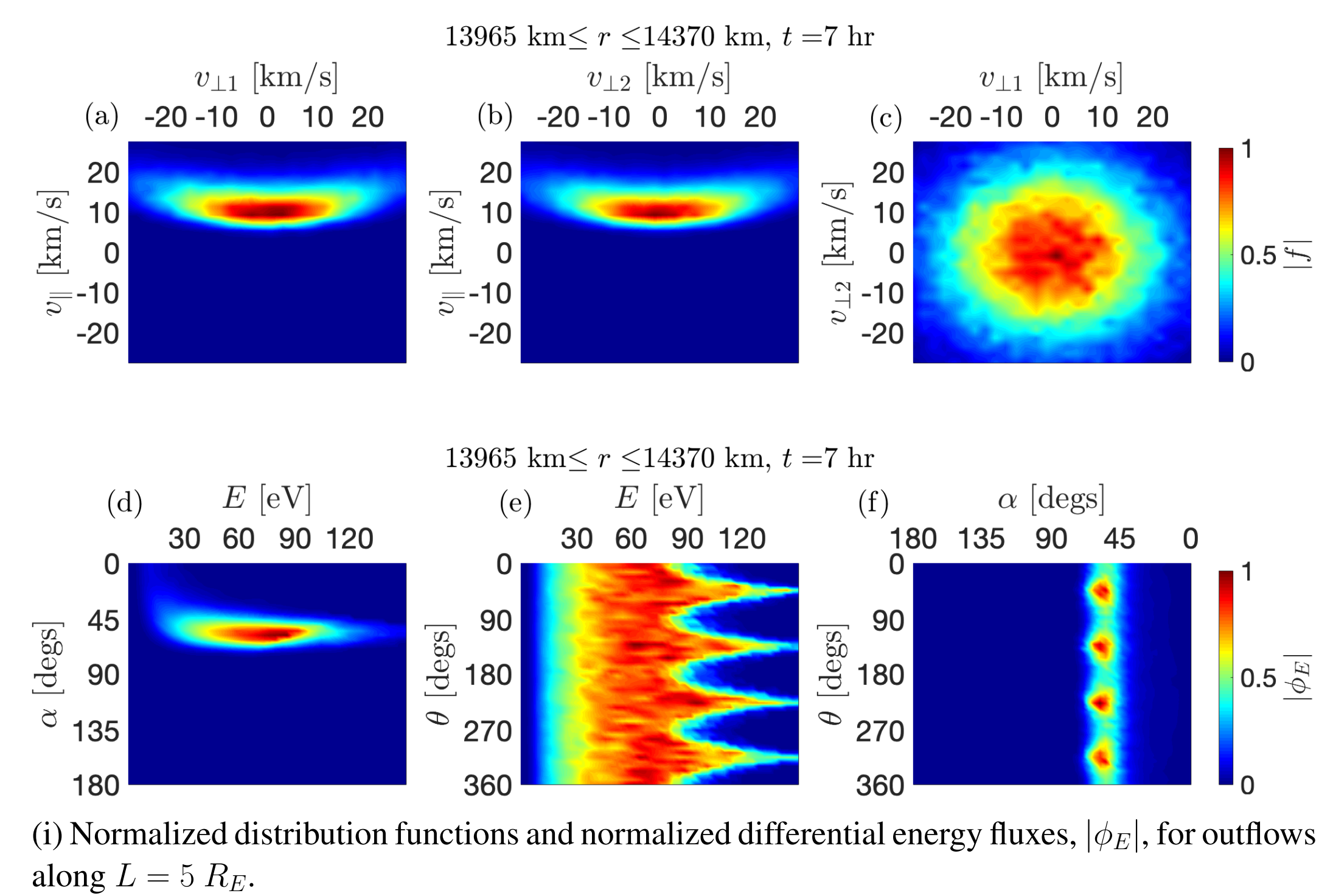


(e) Velocity-space distributions for active ambipolar electric field spin-up. (f) Energy-pitch-angle distributions for active ambipolar electric field spin-up.

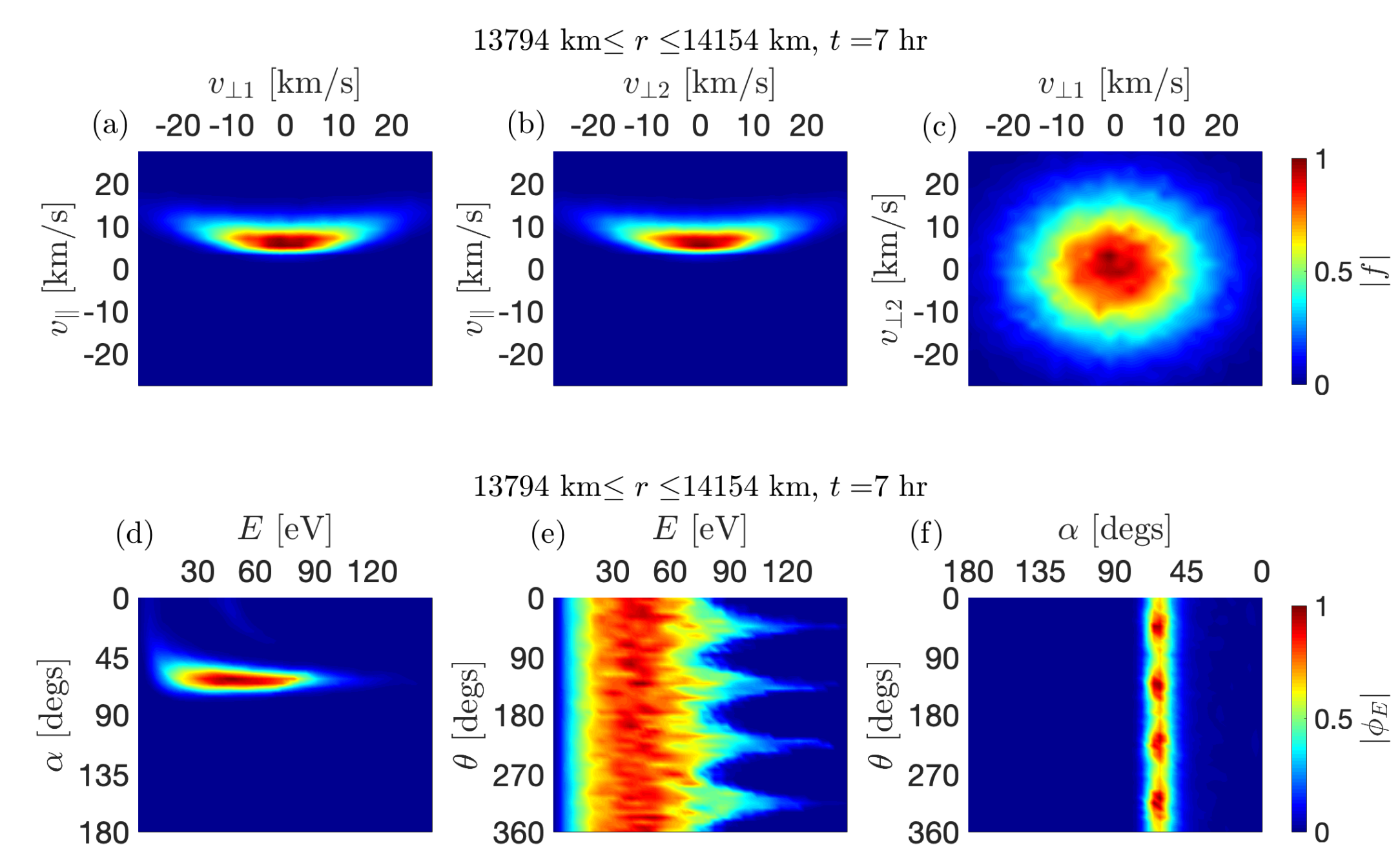
L-SHELL DEPENDENT WAVE HEATING



(g) Outflow moments on $L = 5 R_E$. (h) Outflow moments on $L = 15 R_E$.



(i) Normalized distribution functions and normalized differential energy fluxes, $|\phi_E|$, for outflows along $L = 5 R_E$.

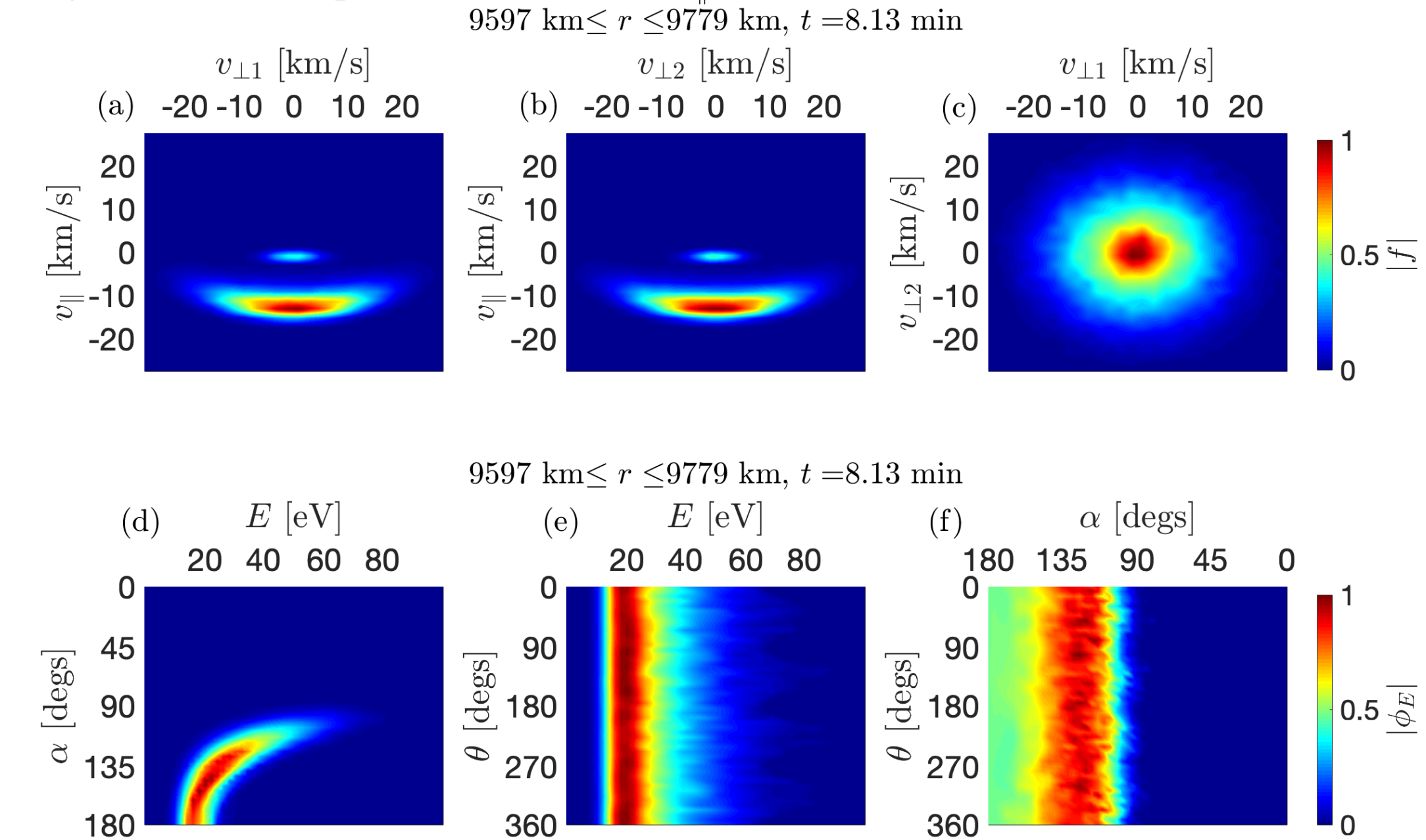


(j) Normalized distribution functions and normalized differential energy fluxes, $|\phi_E|$, outflows along $L = 15 R_E$.

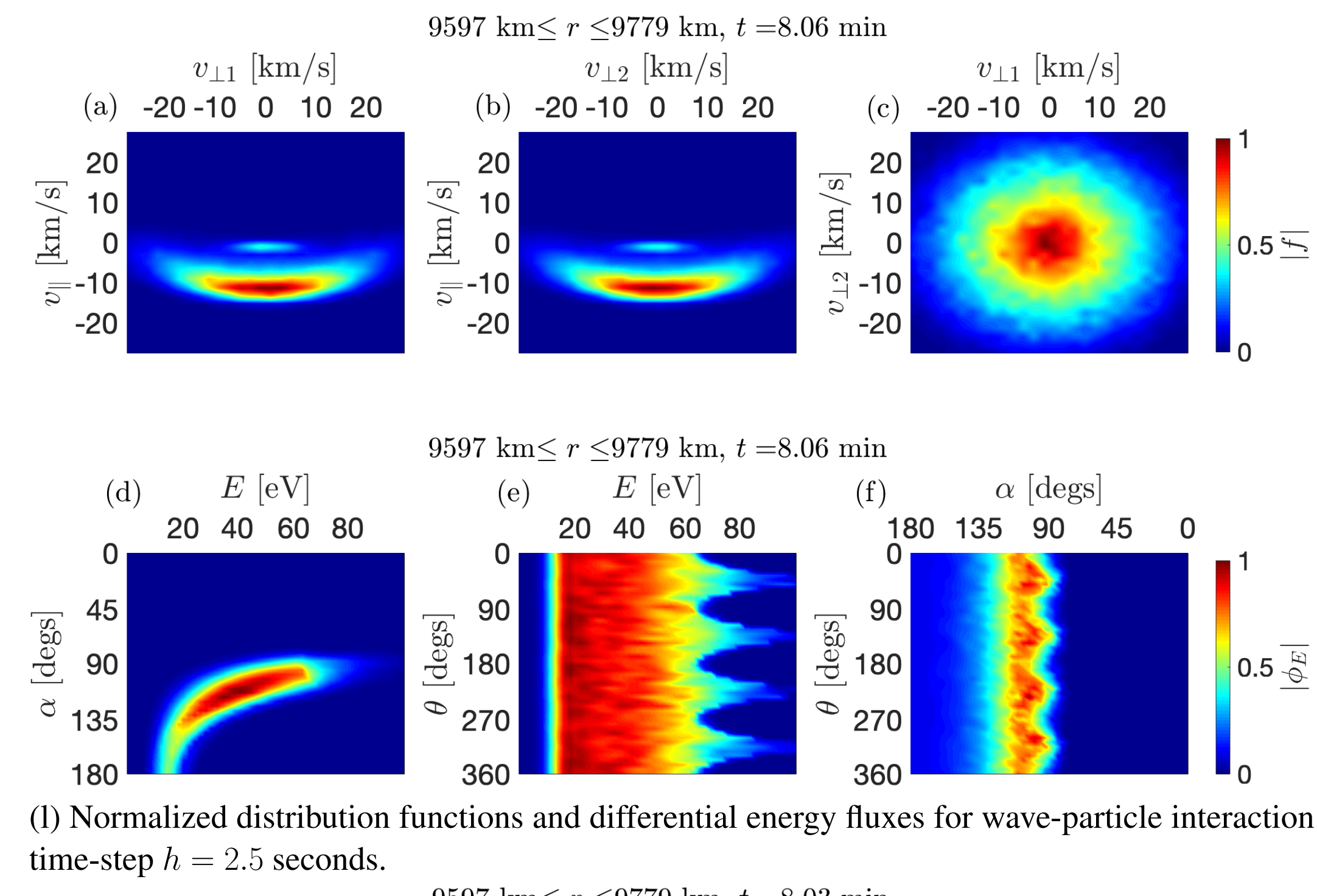
$S_0 = 5 \times 10^{-7} \text{ V}^2 \cdot \text{m}^{-2} \cdot \text{Hz}^{-1}$ at reference gyro-frequency $f_{g0} = 6.5 \text{ Hz}$, spectral index $\chi_{\perp 1} = \chi_{\perp 2} = 2.1$, and ion-turbulence interaction time-step $h = 1.3 \text{ seconds}$. $\eta_{LH} = 0.125$, $\chi_{\perp 1} = \chi_{\perp 2}$, and $\xi_{\perp 1} = \xi_{\perp 2} = 0.5$. At $r \sim 14000 \text{ km}$, the magnetic field strength, and thus gyro-frequency, is greater along $L = 15 R_E$ than for $L = 5 R_E$. At this altitude, the O⁺ gyro-frequency along $L = 15 R_E$ is $f_g \sim 1.67 \text{ Hz}$ and $f_g \sim 1.32 \text{ Hz}$ along $L = 5 R_E$. Due to the strong altitude-dependence of wave spectral density, ions are exposed to greater wave powers along $L = 5 R_E$ than for $L = 15 R_E$ at a given altitude, reference spectral density and frequency, interaction time-step, and spectral index. Outflows on greater L-shells at a given altitude act to subject ions to lower powered waves. Transverse heating rates tend to more readily saturate for outflows along lower L-shell values at a given altitude, heating parameterization, and transverse wavelength.

MAGNETOSPHERIC PRESSURE COOKERS

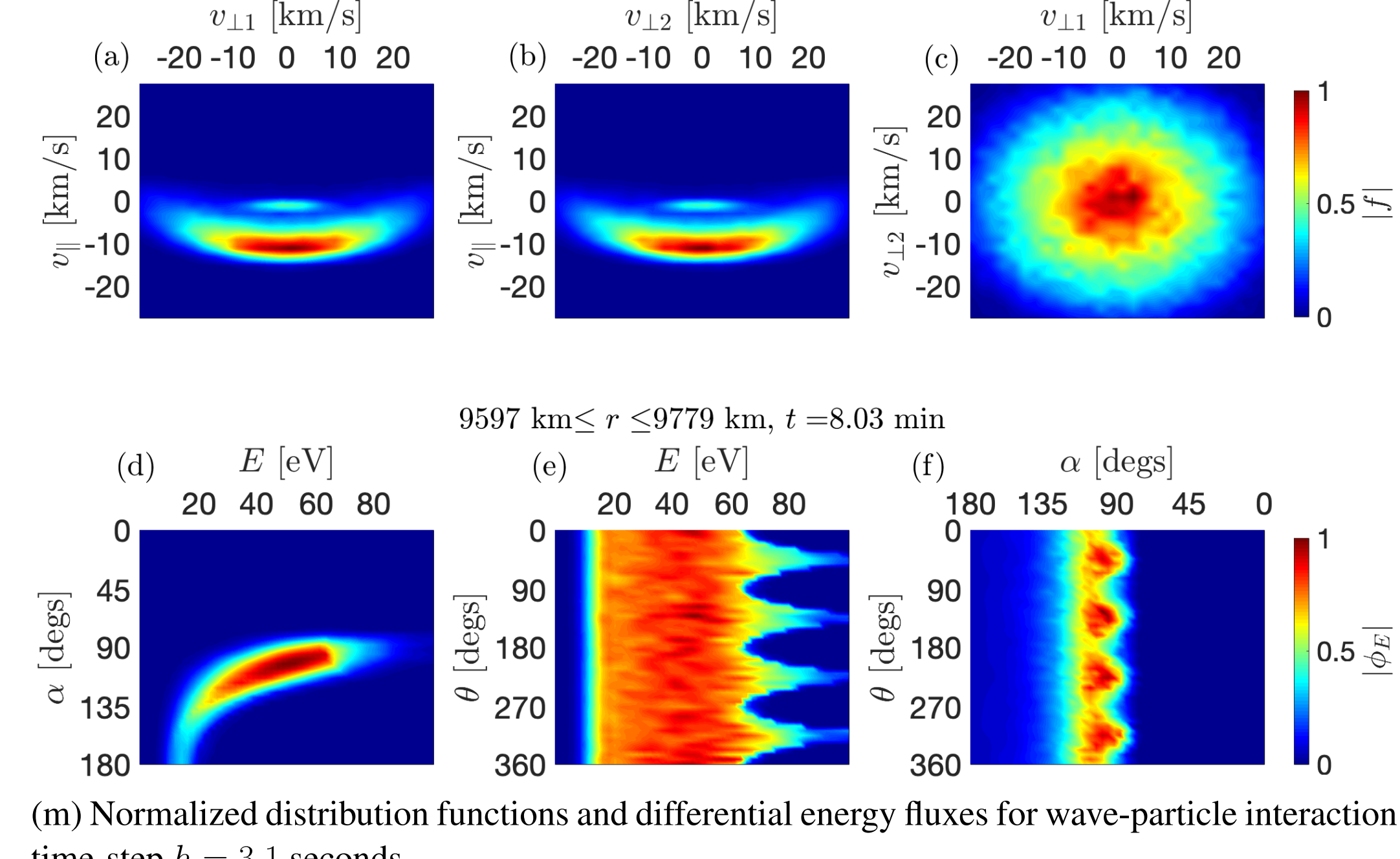
Wave reference power spectral density is $S_0 = 5 \times 10^{-7} \text{ V}^2 \cdot \text{m}^{-2} \cdot \text{Hz}^{-1}$ at reference gyro-frequency $f_{g0} = 6.5 \text{ Hz}$, and wave power spectral index $\chi_{\perp} = 2.1$ in long wavelength regime. Reference parallel electric field $E_{\parallel 0} = 5 \times 10^{-6} \text{ V} \cdot \text{m}^{-1}$.



(k) Normalized distribution functions and normalized differential energy fluxes for wave-particle interaction time-step $h = 1.3 \text{ seconds}$.



(l) Normalized distribution functions and differential energy fluxes for wave-particle interaction time-step $h = 2.5 \text{ seconds}$.



(m) Normalized distribution functions and differential energy fluxes for wave-particle interaction time-step $h = 3.1 \text{ seconds}$.

CONCLUSION

A direct simulation Monte Carlo (DSMC) kinetic model of ionospheric outflows is introduced with numerical investigations of wave-heated outflows along curved magnetic field lines and pressure cooker environments. Plasmas obtain kinetic equilibria as slight departures from hydrostatic solutions, particularly at collision-less altitudes where fluid descriptions break down. Altitude ranges, heating parameters, and reference parallel electric fields of potential structures govern the ascent or descent of energized ion distributions. Magnetospheric pressure cookers may generate descending conics thus transfer transversely energized distributions to lower altitudes. For equivalent heating parameters and altitudes, lower L-shell values expose outflows to higher-powered waves. The parameter space of reference wave power, S_0 , transverse wavelength, λ_{\perp} , ion-turbulence interaction time-step, h , reference parallel electric field, $E_{\parallel 0}$, and potential structure altitude profiles and ranges in actuality vary in space and time to produce various pressure cooker reflection altitudes and parallel energies. Realistic constraints on these parameters must be imposed to computationally describe observations. Low-altitude parallel energetics are governed by synergistic relations between two processes: the transfer of high-altitude ions heated at high-power to low altitudes by strong parallel electric fields, and the ability of particle magnetic moments to adiabatically convert perpendicular to upwards parallel energy. Both mechanisms depend on altitude ranges modeled. Future work includes the exploration of refined parameter-space and further validation studies with in-situ measurements. This provides quantitative means to interpret observational data and related remote sensing approaches to study ion outflows and serves to advance our understanding of drivers and particle dynamics in auroral ionosphere and magnetosphere conditions and to improve data analysis for future sounding rocket and satellite missions.

REFERENCES & ACKNOWLEDGEMENTS

- Albarran, R. M., Zettergren, M., Rowland, D., Klenzing, J., & Clemmons, J., (2024) Kinetic modeling of ionospheric outflows in pressure cooker environments. *Journal of Geophysical Research: Space Physics*, 129, e2023JA031658. <https://doi.org/10.1029/2023JA031658>

This project was supported by NASA grants: NNX15AJ08G and NNX16AF06G and NSF grant: AGS-1255181.

This poster was typeset in L^AT_EX based on the template created by J. Klenzing.

Contact: albarran1@atmos.ucla.edu